Spectrum of Engineering Sciences
ISSN (e) 3007-3138 (p) 3007-312X Volume 3, Issue 5, 2025

COMPRESSIVE ANALYSIS OF MULTI-INFILL LATTICE STRUCTURE PARTS 3D PRINTED BY FDM

Noor Faraz Khan[*1], Dr. Abdul Shakoor[2], Muhammad Bilal Afzal[3], Atif Shehzad[4]

[*1,2]*University of Engineering & Technology, Peshawar*
[3]*Pakistan Council of Scientific & Industrial Research*
[4]*NED University of Engineering & Technology*

DOI: https://doi.org/10.5281/zenodo.15478686

Keywords
Fused Deposition Modeling (FDM), PLA+, Multi-Infill, Gyroid, Cubic, Lattice Structures, Additive Manufacturing.

Article History
Received on 13 April 2025
Accepted on 13 May 2025
Published on 21 May 2025

Corresponding Author: *
Noor Faraz Khan

Abstract
This study investigates the failure mechanisms of multi-infill lattice structures fabricated using Fused Deposition Modeling (FDM) under compressive loading. Leveraging a combination of Gyroid and Cubic infill geometries, seven stacking configurations—including both pure and hybrid designs—were 3D printed using PLA+ material. The mechanical performance and failure modes of these configurations were evaluated through standardized compression tests, following ASTM D695 guidelines. Results reveal that stacking sequence, interlayer transitions, and pattern geometry significantly influence the mode and progression of failure. Specimens with Gyroid infill exhibited progressive and ductile failure, while Cubic-dominant designs failed in a brittle and localized manner. Hybrid patterns, particularly those with alternating Gyroid-Cubic layers, showed a combination of ductile and brittle failure characteristics. The study provides critical insights into the design of structurally resilient components for engineering applications requiring high compressive strength and energy absorption

INTRODUCTION

Additive Manufacturing (AM), widely recognized as 3D printing, has significantly transformed the modern manufacturing landscape by enabling the production of complex geometries directly from digital models. Among various AM techniques, Fused Deposition Modeling (FDM) stands out for its cost-effectiveness, material versatility, and ease of use [1]. It has become the preferred method for producing functional prototypes, tools, and even end-use parts in industries ranging from aerospace and automotive to healthcare and consumer products [2].

However, one of the persistent limitations of FDM is the relatively poor mechanical performance of the printed parts, particularly under mechanical loads such as tension, compression, and impact[3]. This drawback is especially pronounced in structural and load-bearing applications, where high strength and stiffness are essential. To address these issues, the internal architecture—specifically, the infill pattern—of FDM-printed parts has gained considerable attention as a design variable to enhance mechanical performance [4].

The infill structure, which constitutes the internal volume of a printed component, plays a pivotal role in determining its mechanical properties[5]. Traditional FDM printing commonly uses a single infill pattern throughout the part, which limits the scope of performance optimization [6]. In contrast, multi-infill lattice structures, which integrate two or more infill geometries within a single part, offer a promising approach to tailoring mechanical behavior by regionally varying stiffness, strength, and energy absorption [7].

Among the various infill patterns, Gyroid and Cubic geometries are widely studied due to their contrasting mechanical characteristics. The Gyroid pattern, based on a triply periodic minimal surface (TPMS), provides isotropic strength and excellent energy dissipation. Conversely, the Cubic pattern offers higher stiffness in specific orientations but tends to exhibit anisotropic and brittle failure under load. When strategically combined, these patterns can complement each other to produce optimized hybrid structures with enhanced compressive performance [8].

Despite numerous computational studies on lattice and infill design, experimental investigations on the compressive failure modes of multi-infill structures, particularly using PLA+ material in FDM, remain limited [9]. Understanding how infill stacking sequences influence failure initiation, progression, and overall compressive strength is essential for advancing FDM into more demanding applications [8].

The primary aim of this research is to analyze the compressive failure mechanisms of PLA+ multi-infill lattice structures fabricated using FDM technology[10]. The study seeks to address the following objectives:

- To investigate the compressive strength and failure modes of various multi-infill stacking sequences composed of Gyroid and Cubic geometries.
- To compare the performance of multi-infill structures with pure single-infill counterparts.
- To evaluate how pattern transitions and interlayer interfaces influence stress concentration and fracture propagation.
- To identify design strategies that can optimize compressive strength, energy absorption, and structural integrity in 3D-printed parts.

By systematically studying the compressive failure behavior of multi-infill PLA+ lattice structures, this research provides valuable insights for design engineers and manufacturers aiming to enhance the structural performance of FDM-printed components. The findings contribute to the growing body of knowledge on infill optimization, offering experimental evidence that supports the adoption of hybrid infill strategies in lightweight, high-strength, and load-bearing applications.

2. Methodology

2.1 Specimen Design and Fabrication

Seven different infill stacking sequences were designed using SolidWorks and fabricated on a Creality Ender 3 V3 SE FDM printer as shown in Figure 2.1. All samples were printed using PLA+ at a constant infill density of 60% and specification shown in Table 2.1. The stacking sequences are demonstrated in Table 2.2.

Figure 2.1: Creality Ender 3 V3 3D printer

Table 2.1: Sets of used process parameters

Description	Specification
Material	PLA+
Layer height (mm)	0.1
Wall line count	2
Top/Bottom thickness (mm)	0.2
Top/Bottom layer (mm)	0.2
Infill density	60%
Infill layer thickness (mm)	0.2
Bed temperature (°C)	70
Nozzle temperature (°C)	210
Printing speed (mm/s)	40
Retraction distance (mm)	5
Retraction speed (mm/s)	45

Table 2.2: Description of multi-infill stacking sequences and pure infill

S.No	Stacking Sequence	Designation	Description
1	S1	G	Entire specimen fabricated with Gyroid pattern
2	S2	CG	Specimen divided into two equal sections, one section fabricated with Gyroid and the other with Cubic pattern i,e 50% Gyroid ,50%Cubic)
3	S3	GCG	Specimen divided into three equal sections, alternating between Gyroid and Cubic i,e 33.33% Gyroid, 33.33% Cubic, 33.33% Gyroid
4	S4	CGC	Specimen divided into three equal sections, alternating between Cubic and Gyroid i,e 33.33% Cubic, 33.33% Gyroid, 33.33% Cubic
5	S5	CGCGC	Specimen divided into five equal sections, starting and ending with Cubic (20% Cubic alternating with 20% Gyroid)
6	S6	GCGCG	Specimen divided into five equal sections, starting and ending with Gyroid (20% Gyroid alternating with 20% Cubic)
7	S7	C	Entire specimen fabricated with Cubic pattern

The specimens were designed and fabricated in compliance with the ASTM D695 standard [11] as illustrated in Figure 2.2. The design process was carried out using SolidWorks 2022 software, and the designs were converted to STL files for slicing in Ultimaker Cura. The sliced files were then used to fabricate the specimens on the Creality Ender V3 SE 3D printer. Each sequence was fabricated in triplicate to ensure statistical validity.

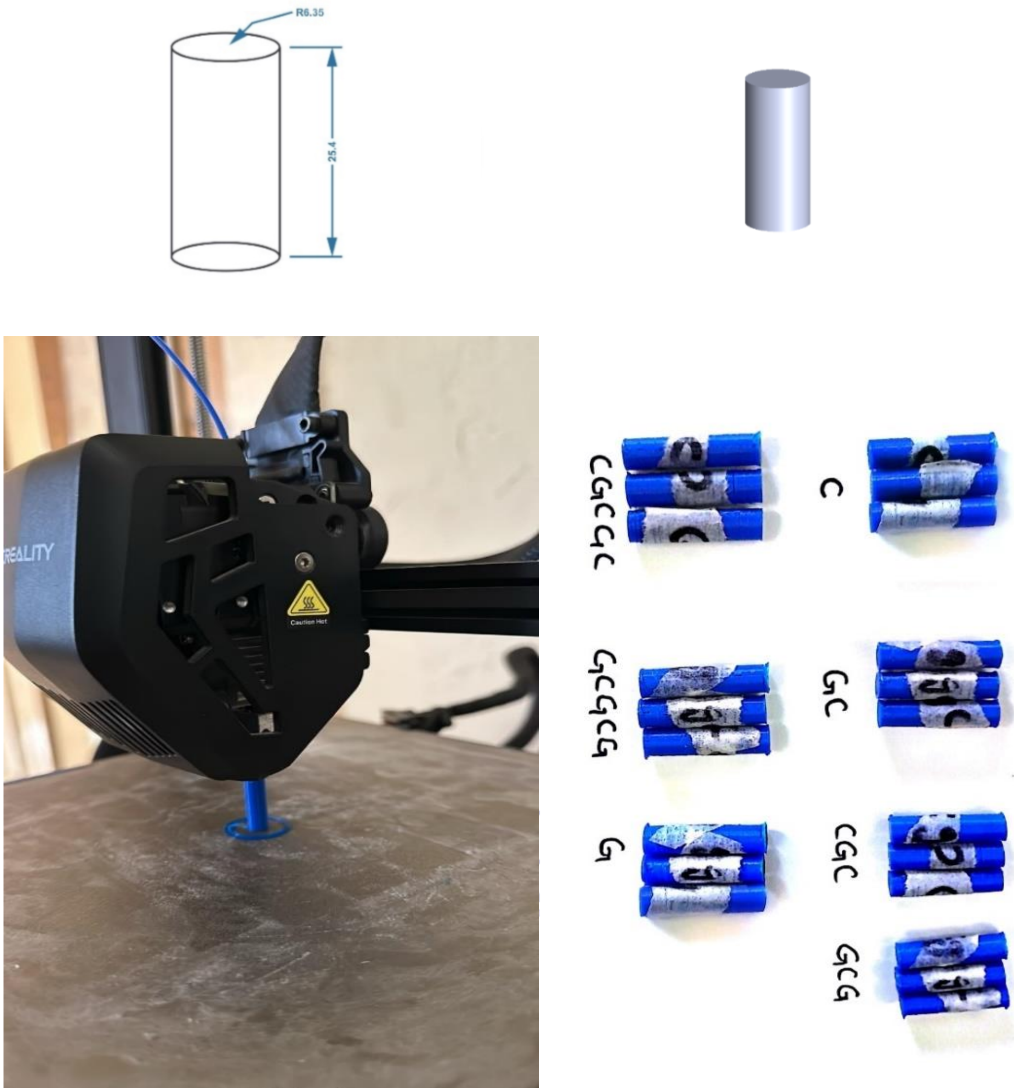

Figure 2.2: CAD model and 3D printed specimen

2.2 Compression Testing

Compression testing was performed as per ASTM D695 [12] standards using a Shimadzu Autograph Universal Testing Machine as illustrated in Figure 2.3. Tests were conducted at room temperature with a constant loading rate until structural failure occurred. Data on load, displacement, and stress were recorded in real-time. The primary metrics evaluated included maximum compressive stress, load capacity, and failure morphology. Observations during testing and post-failure inspections were used to identify dominant failure modes for each configuration.

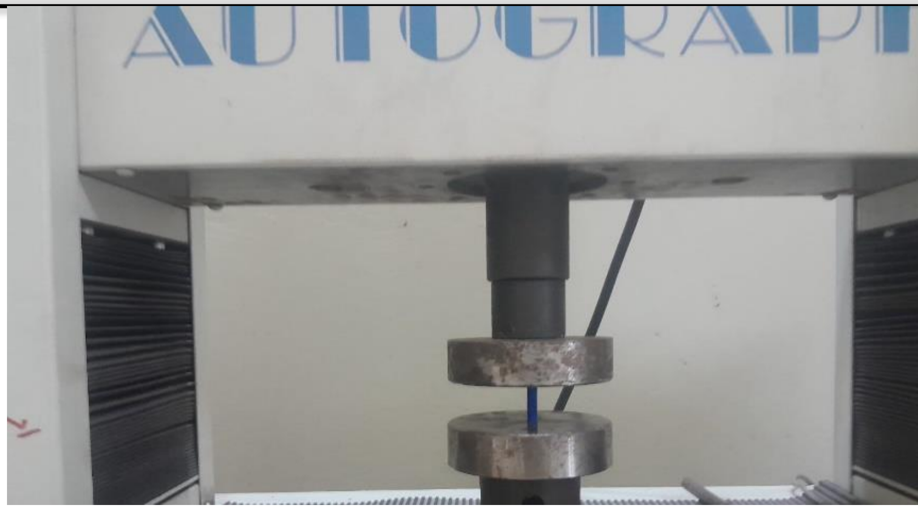

Figure 2.3: UTM Setup for compression test

3. Results and Observations 3.1 Compressive Strength Performance

The compressive strength results showed clear differences among the stacking sequences as illustrated in Figure 3.1 and Table 3.1.

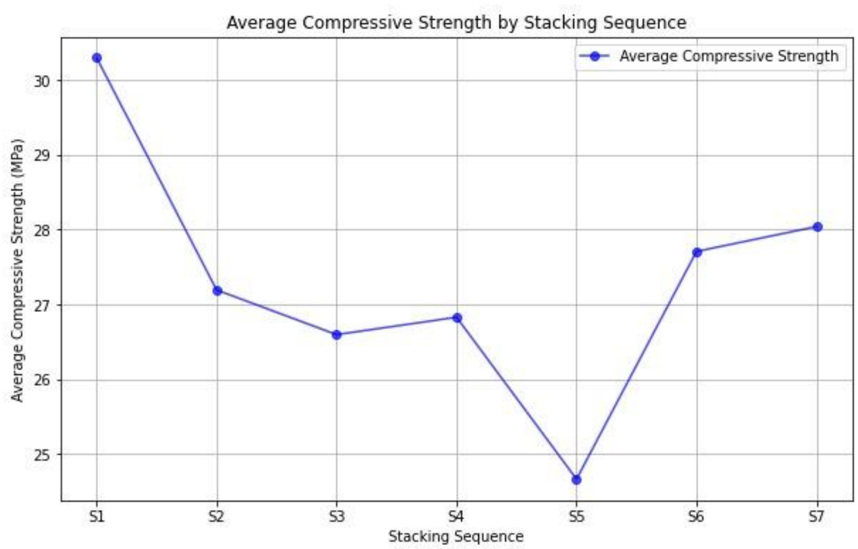

Figure 3.1: Average Compression Strength of all stacking sequences

Table 3.1: Average Max Stress and Load against each sequence

S.No	Stacking Sequence	Max Stress	Max Load	Strength to weight ratio
1	S1	30.3 ±0.2	3837.5	10.74
2	S2	27.18 ±0.1	3443.752	9.48
3	S3	26.59 ±0.7	3368.752	9.43
4	S4	26.79 ±0.2	3393.752	9.31
5	S5	24.5 ±0.07	3289.6	8.52
6	S6	27.72 ±0.1	3512.5	9.72
7	S7	28.02 ±0.06	3550	9.63

The Gyroid pattern's smooth curvature distributed loads uniformly, resulting in the highest compressive strength. In contrast, frequent transitions in hybrid sequences such as S5 contributed to stress concentration, reducing strength.

3.2 Observed Failure Modes

Following failure mode was observed

Stacking Sequence	Failure Mode Characteristics
S1 (Gyroid)	Progressive, ductile buckling across curved walls
S7 (Cubic)	Brittle, sudden fracture with sharp crack propagation
S2 (GC)	Mixed-mode: ductile in Gyroid layers, brittle in Cubic
S3/S4	Moderate deformation, localized interfacial failures
S5/S6	Stress concentration at pattern interfaces, delamination observed

3.3 Fracture Surface and Visual Inspection

Post-test inspection revealed the following key failure features:

- Gyroid sections showed distributed deformation with visible wall buckling.
- Cubic regions failed by clean fracture lines aligned with raster orientation.
- Interfaces between infill types exhibited delamination or micro-cracking.
- The degree of deformation was higher in Gyroid-dominant sections, indicating better energy absorption.

4. Discussion

4.1 Influence of Infill Geometry

Gyroid patterns, due to their triply periodic minimal surface (TPMS) nature, promote uniform stress distribution and absorb compressive energy more efficiently. In contrast, Cubic infill tends to behave more rigidly, focusing stress along straight-line paths, which results in localized failure.

4.2 Role of Stacking Sequences and Transitions

Hybrid sequences combine the advantages of both patterns but introduce weaknesses at transition layers. Sequences with fewer transitions (e.g., S2) maintain better structural continuity and load-sharing. However, sequences like S5, with multiple transitions, showed premature failure due to weak interfacial bonding and abrupt changes in mechanical behavior [13].

4.3 Practical Implications

Understanding the failure behavior of these multi-infill structures provides valuable design insights for load-bearing applications. For instance, components requiring progressive collapse and energy absorption (e.g., protective gear, automotive crumple zones) may benefit from Gyroid-rich or hybrid infills like S6. Conversely, for parts needing rigidity, such as structural brackets, Cubic patterns may still be favorable.

5. Conclusions T

This study confirms that infill geometry and stacking sequence significantly influence the compressive behavior and failure modes of PLA+ 3D printed parts:

- Gyroid infill offers superior compressive performance due to isotropic energy distribution.
- Cubic infill fails abruptly, with higher stiffness but reduced energy absorption.
- Hybrid stacking can optimize both properties but requires careful transition design.
- Frequent pattern shifts (as in S5) lead to stress concentrations and premature failure.

6. Future Work

Future research should consider:

- Gradient infill transitions to reduce interfacial stress.
- Application of high-performance thermoplastics or composites.
- Use of simulation tools (e.g., FEA) to predict stress zones and improve design.
- Study of fatigue and cyclic loading for real-world applicability.
-

REFERENCES

1. Pande, S., et al., Selection of Selective Laser Sintering Materials for Different Applications. Rapid Prototyping Journal, 2015. **21**: p. 631-638.
2. Shahrubudin, N., L. Te Chuan, and R. Ramlan, An Overview on 3D Printing Technology: Technological, Materials, and Applications. 2019. **35**: p. 1286-1296.
3. Imran, M.M.a., et al., Advancements in 3D Printing: Directed Energy Deposition Techniques, Defect Analysis, and Quality Monitoring. Technologies, 2024. **12**(6): p. 86.
4. Nagaraju, D.S., et al., Mechanical properties of 3D printed specimen using FDM (Fused deposition modelling) and SLA (Stereolithography) technologies. Materials Today: Proceedings, 2023.
5. Kumaresan, R., et al., Fused deposition modeling: process, materials, parameters, properties, and applications. The International Journal of Advanced Manufacturing Technology, 2022. **120**.
6. Kristiawan, R.B., et al., A review on the fused deposition modeling (FDM) 3D printing: Filament processing, materials, and printing parameters. Open Engineering, 2021. **11**(1): p. 639-649.
7. Naik, M., D.G. Thakur, and S. Chandel, An insight into the effect of printing orientation on tensile strength of multi-infill pattern 3D printed specimen: Experimental study. Materials Today: Proceedings, 2022. **62**: p. 7391-7395.
8. Dey, A. and N. Yodo, A Systematic Survey of FDM Process Parameter Optimization and Their Influence on Part Characteristics. Journal of Manufacturing and Materials Processing, 2019. **3**: p. 64.
9. Gopi Mohan, R., et al., Comparitive analysis of mechanical properties of FDM printed parts based on raster angles. Materials Today: Proceedings, 2021. **47**: p. 4730-4734.
10. Nabavi-Kivi, A., M.R. Ayatollahi, and N. Razavi, Investigating the effect of raster orientation on fracture behavior of 3D-printed ABS specimens under tension-tear loading.
11. International, A., Standard Test Method for Compressive Properties of Rigid Plastics. 2023, ASTM International
12. Pi, Y., et al., Crack propagation and failure mechanism of 3D printing engineered cementitious composites (3DP-ECC) under bending loads. Construction and Building Materials, 2023. **408**: p. 133809.
13. Rajpurohit, S. and H. Dave, Impact strength of 3D printed PLA using open source FFF-based 3D printer. Progress in Additive Manufacturing, 2021. **6**.

.